3D-BLUE: Backscatter Localization for Underwater Robotics

Sayed Saad Afzal[1], Weitung Chen[1], Fadel Adib[1,2]

Confidential – Please do not Distribute

***Abstract*— We present the design, implementation, and evaluation of 3D-BLUE, an ultra-low-power underwater 3D localization system that can be deployed on compact robots to accurately localize them in shallow underwater environments. 3D-BLUE's design introduces two core components. First, it adapts a recent ultra-low-power underwater acoustic communication technology (called piezo-electric backscatter) to the underwater robotics localization problem; specifically, it integrates backscatter nodes into the underwater robot and uses them for localizing it. Second, it leverages the physical properties of the backscatter technology to efficiently extract spatio-temporal-spectral features from the backscatter signal; using these features, it devises a particle-filter-based algorithm to localize the corresponding robot accurately in challenging shallow-water environments. We implemented an end-to-end prototype of 3D-BLUE on a BlueROV2 robot and custom-built backscatter localization system, and evaluated it in dozens of experimental trials in a pool. Our results demonstrate that 3D-BLUE can localize the robot with an accuracy of around 0.25m at close range and an accuracy of around 1.4m at a range of 10m. This high localization accuracy opens important commercial, naval, and environmental applications in challenging shallow-water environments such as shores, rivers, pools, and narrow waterways.**

I. INTRODUCTION

The past few years have witnessed exponential growth in commercial underwater robotics, whose market size is expected to rise to 3.5 billion dollars by 2028 [1]. This growth has been propelled by the decrease in cost, power, and size of underwater drones, which opened up new commercial, scientific, and naval applications. The relatively compact size and power of these robots have made them desirable for deployments in shallow-water environments, such as navigating narrow waterways for the navy; performing infrastructure inspections in pools, waterparks, and bays; and environmental monitoring for near-coast habitats, coastal resilience, and seafood production (offshore aquafarms) [2], [3], [4], [5].

A key problem for this emerging class of subsea drones is localization. While underwater localization is a classical problem in marine robotics, the compact form factors and new deployment environments for these drones pose new challenges. In particular, the most common approach for underwater robot localization relies on acoustic beacons (such as LBL, SBL, and USBL systems) [6], [7], [8]. In these systems, an acoustic transceiver on the underwater drones leverages the deployed beacons for localization. However, existing approaches do not meet the accuracy, power budget, and cost requirements of compact underwater drones. In terms of accuracy, most of these systems achieve tens or hundreds of meters of location accuracy, which is suitable for the open ocean, but not for narrow waterways, coastal environments, or commercial pools (e.g., for infrastructure inspection). While some of the existing systems have higher resolution (e.g., sub-meter), they struggle to maintain this accuracy in shallow-water environments due to significant acoustic reflections from the seabed and surface[8], [9], [10], [11].

These authors are with [1] *Massachusetts Institute of Technology,* [2] *Cartesian Systems*, (email: afzals, weitung, fadel@mit.edu).

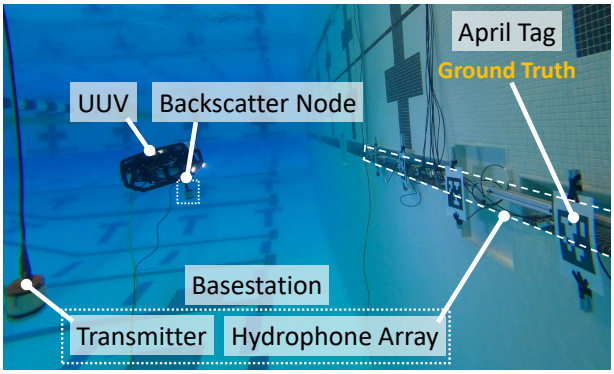

Fig. 1: **Underwater Bacskcatter Localization**. The figure shows the end-to-end system design for 3D-BLUE . A backscatter node is mounted on an UUV that bacskcatters the signals produced from the transmitter. A hydrophone array receives the signals to perform localization. April tags are used for ground truth location estimation

The poor accuracy of existing systems is exacerbated by their cost and power requirements. For example, while the price of a single USBL system (around $7K [12]) is negligible for classical underwater drones (which cost tens to hundreds of thousands of dollars), it is significant for many compact underwater drones, which cost less than $1K [13]. Furthermore, due to the power consumption of their acoustic transmissions, the beacons often require frequent battery replacement [9], which increases their cost and maintenance overhead.

In this paper, we ask whether it is possible to develop a novel low-power, low-cost underwater localization method tailored to this emerging class of underwater drones. Ideally, such a localization system would consume only a fraction of the power and cost of these drones. Moreover, it would be capable of accurate localization (sub-meter accuracy) in the expected shallow water environments. Achieving these goals is challenging not only due to the power, cost, and size constraints but also due to the significant acoustic reflections off the seabed and water surface that make it difficult to associate the acoustic signal with its source direction.

We present 3D-BLUE (3D **B**ackscatter **L**ocalization for **U**nderwater **E**nvironments) which is a compact, ultra-low power localization module that can be directly integrated onto the robot and enables localizing them in shallow

underwater environments (shown in Fig.1). Our approach leverages a recent networking technology called underwater backscatter, which consumes sub-milliWatt power [14]. Past research has demonstrated the effectiveness of underwater backscatter for communication, but leveraging it in localization and navigation remains an open problem. We envision integrating ultra-low-power backscatter nodes into compact underwater drones to localize them in rivers, lakes and pools. Such localization can be performed remotely from a base station near shore/poolside or attached to the bottom of a surface vessel, e.g. a ship.

Utilizing underwater backscatter for localization in shallow-water environments presents multiple challenges. Current state-of-the-art underwater localization systems rely on computing the time-of-arrival (ToA) [6], [7]. In these systems, a transceiver emits an acoustic pulse and awaits a response from the transponder beacon. The time difference between the initial pulse and the reply is used to determine the distance between the two nodes (by multiplying it with the sound speed in water). However, this ToA estimation technique does not work with underwater backscatter nodes in shallow water environments. This is because when acoustic signals travel in these environments, they repeatedly bounce back and forth between the seabed and the water surface before arriving at a receiver. Such dense multipath reflections distorts the acoustic signals and make it difficult to associate them with their source to estimate ToA.

To address these challenges, 3D-BLUE exploits the fundamental physical properties of underwater backscatter to enable accurate localization. Unlike traditional underwater acoustic communication systems, where each node generates its own signals, backscatter nodes communicate by reflecting acoustic signals in the environment (more specifically modulating the reflections using a code). 3D-BLUE exploits this property to extract rich spatio-temporal-spectral (space, time, and frequency) features from the backscatter reflection for localization. In particular, it leverages a helper base station that transmits signals of different frequencies and captures the reflections from different spatial positions. The combination of these features enables 3D-BLUE to perform real-time localization even in environments with severe multipath. 3D-BLUE improves the localization accuracy by employing a particle filter-based algorithm, tailored to the acoustic reflections in these environments. Furthermore, because backscatter is ultra-low-power, the power consumption of these nodes is neglible with respect to that of the low-power underwater drone.

This paper provides three main contributions:

- It presents the first ultra-low power system that can perform 3D localization using underwater backscatter.
- It introduces a particle filter-based algorithm that exploits the spatio-temporal-spectral features for robust localization in shallow water environments and under mobility.
- It presents an end-to-end prototype implementation and evaluation of 3D-BLUE . The implementation is built using a BlueROV robot, mechanically fabricated backscatter node and custom-built base station (consisting of a projector and a multichannel receiver array with 8 hydrophones). The system is evaluated in over 1900 locations and compared to an Apriltag-based ground truth location baseline. The evaluation demonstrates that 3D-BLUE can localize a backscatter node with an accuracy of around 0.25m at close range and an accuracy of around 1.4m at a range of 10m. Moreover, it demonstrates that 3D-BLUE can localize accurately in the presence of motion with an accuracy of around 0.25m when the node is moving with a speed of 0.1m/s.

While we demonstrated the performance of our system on a BlueROV robot with a reasonably good power budget (around 275W), in practice, it can also be extended to low-power robots which have even more limited onboard power [15], whereby the sub-milliWatt power consumption of underwater backscatter would remain negligible. Moreover, each underwater backscatter node can be fabricated at a cost less than $100 [14], making them much more cost-effective than existing underwater localization systems.

II. RELATED WORK

Past work in underwater drone localization and navigation includes acoustic and non-acoustic methods, described below.

Acoustic Underwater Localization. Conventional underwater localization systems primarily rely on deploying beacons in the ocean and using their signals for localization. Earlier methods used the received signal strength (RSSI) or the angle-of-arrival (AoA) to perform triangulation or trilateration[16], [17]. State-of-the-art underwater localization systems, known as Long Baseline (LBL), Short Baseline (SBL), and Ultra-Short Baseline (USBL) methods [6], [7], [8], employ ToA-ranging techniques. These systems utilize transceivers to emit pulses on the downlink and transponders to receive and respond with pulses for ToA estimation. While these systems perform well in the deep ocean, the accuracy of these systems is compromised by severe multipath interference, limiting their functionality in shallow underwater environments [8], [9], [10], [11]. Moreover, these systems depend on generating acoustic pulses from the transponders, each consuming approximately 25W [18], [19], [20]. This power consumption can significantly deplete a drone's battery, which makes them undesirable for low-power robots.

To address the issue of multipath, researchers have also explored methods for performing underwater localization in shallow water environments. For instance, one approach involves deploying a large number of nodes or drones and combining the data from them to eliminate the impact of multipath using geometry [21]. Other methods rely on fingerprinting techniques via bathymetry, pattern matching, or underwater waveguide channel models to address multipath issues [22], [23], [24]. However, these systems make unrealistic assumptions that are difficult to implement in practice: while some of them assume that the entire underwater channel is known apriori, others require the deployment of hundreds of nodes which is not feasible or cost-effective in real-world settings.

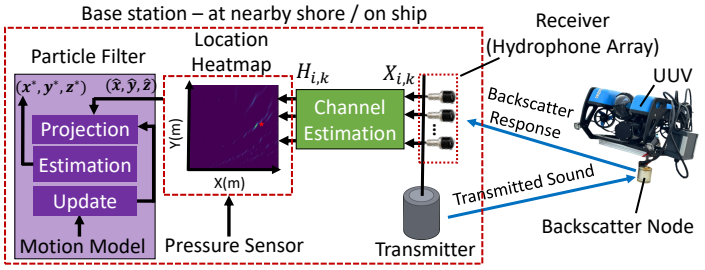

Fig. 2: **3D-BLUE E2E System.** The figure shows the end-to-end system for 3D-BLUE. The base station transmits sound and receives the backscatter response $X_{i,k}$. It computes the channel estimate $H_{i,k}$ to generate the location probability heat map which is improved via a particle filter to obtain the final location estimate (x^*, y^*, z^*)

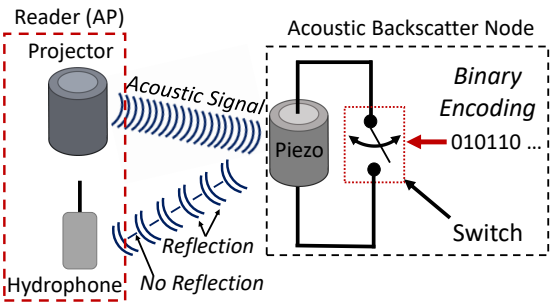

Fig. 3: **Piezo-Acoustic Backscatter.** A node communicates bits of zero and one by switching the impedance control.

3D-BLUE shares the motivation of these systems but it is the first system that enables practical and low-power underwater acoustic localization in shallow environments. It does so using backscatter which consumes much less power (sub-milliWatt) compared to a few tens of watts power consumption of traditional acoustic localization systems. In doing so, it builds on recent research that demonstrated the feasibility of using backscatter in 1D localization at close distances ($\leq$1m) [25], and is the first to demonstrate accurate 3D backscatter-based localization for underwater robotics at decimeter ranges.

Non-Acoustic Underwater Localization. Previous research has explored alternative methods for underwater positioning beyond acoustics, including visual odometry and geomagnetism [26], [27], [28], [29]. However, geomagnetism suffers from poor localization accuracy (approximately 100m) due to fluctuating magnetic fields. Visual odometry can achieve high accuracy in clear waters but suffers in turbid environments and is prone to long-term drift. Despite attempts to mitigate drift through SLAM models, these solutions demand significant computational power, often unavailable on energy-constrained AUVs [30]. In contrast, 3D-BLUE can work well in turbid environments, similar to typical underwater acoustic localization methods, and it can do so in shallow-water and at low-power.

III. SYSTEM OVERVIEW

The primary objective of 3D-BLUE is to localize underwater robots in shallow-water environments. In a typical deployment scenario, we envision integrating a backscatter node onto the robot/drone, while a base station is at nearby shore or ship to localize the drone as shown in Fig. 2. The base station estimates the drone's location, which can be directly utilized in diverse applications (e.g., to understand where footage from the drone is being captured for infrastructure/environmental/naval monitoring). Moreover, if the drone requires its location (e.g., for navigation), the base station may transmit it to the drone through a standard acoustic link.

A. Primer on Underwater Backscatter

Before describing 3D-BLUE's localization algorithm, we provide a brief background of underwater backscatter and refer the interested reader to past work for more details [14]. Underwater backscatter nodes are piezoelectric transducers that communicate by reflecting rather than generating acoustic signals. Fig. 3 depicts the basic operation of this communication technology focusing on a single backscatter node (the same can be extended to a network [14]). In these systems, the base station transmits sound, and the backscatter node communicates by reflecting (modulating) the sound. Specifically, by switching between reflective and non-reflective states, the node encodes its data in binary, and the changes in reflections can be decoded by a remote receiver (hydrophone).

Underwater localization requires estimating the path between the backscatter node and the receiver. By estimating this path, one could apply different localization techniques such as computing the angle (for triangulation) or the distance (for trilateration). To estimate the path, the receiver needs to extract features from the received signal that come from its propagation underwater. These features are encoded in what is typically called the *underwater backscatter channel*.

This channel can be extracted using standard communication techniques [31]:

$$h(X) = H = \frac{1}{T}\sum_{t \in T} X(t)p^*(t) \quad (1)$$

where X is the received signal, p is the known transmitted signal (from the backscatter node), and $h(.)$ is a function that maps the received signal X to the corresponding channel H. t and T denote time and the period for the transmitted signal p.

B. Problem Definition

3D-BLUE's goal is to estimate the 3D position of the robot from the backscatter response, which is received by one or more hydrophones as shown in Fig. 2. More formally, it aims to solve the following optimization problem:

$$p_{node}(\hat{x}, \hat{y}, \hat{z}) = \arg\max_{(x,y,z)} g(h(X)) \quad (2)$$

where *g(.)* is a function that combines spatio-temporal-spectral features from the channel and outputs a probability heatmap of the node's location. 3D-BLUE uses this information to estimate the corresponding robot's location.

C. Backscatter Localization in Multipath Free Environments

A classical approach for underwater localization is to perform angle-of-arrival (AoA) estimation using multiple hydrophones. At a high level, a receiver combines the

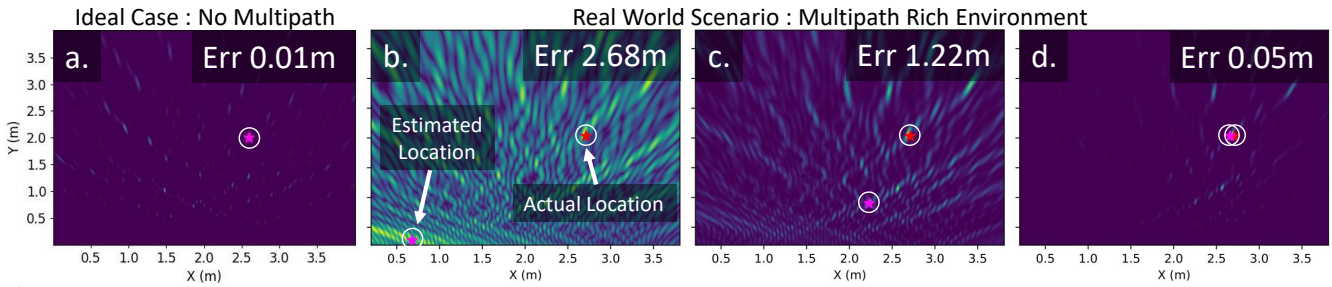

Fig. 4: **3D-BLUE Localization Parameters.** The figure plots the probability of UUV at the corresponding locations as a heatmap in 2D space, where yellow and purple correspond to higher and lower power respectively. The red and pink stars represent the actual and estimated locations. (a) shows a simulated case with a single frequency, 8 hydrophones, and no multipath. (b),(c) and (d) represents a real scenario where 8 hydrophones are used with 1,3 and 6 frequencies to perform localization in the presence of multipath. The error in localization is shown in the top right corner.

received signals from multiple hydrophones and uses them to estimate the angle to the acoustic source. This approach can also be used to perform 2D localization by either combining two hydrophone arrays or performing non-linear array processing [32]. This AoA estimation approach can be applied to underwater backscatter using a receiver array, by operating on the estimated channel at a single frequency H obtained from Eq. 1. Mathematically, we can formulate this as:

$$p_{node}(x,y,z) = \arg\max_{(x,y,x)} \left|\left| \frac{1}{N} \sum_{i=1}^{N} H_i e^{\frac{-j2\pi d_i(x,y,z)}{\lambda}} \right|\right| \quad (3)$$

where λ is the wavelength of the sound frequency, N denotes the number of hydrophones used, H_i is the channel measurement of the i^{th} hydrophone and d_i is the total round-trip distance traveled by the signal from the transmitter to the backscatter node and back to the i^{th} hydrophone.

We simulated such backscatter localization by transmitting a single frequency and using 8 hydrophones separated by 0.56cm to understand the performance of this method in the absence of multipath (i.e., similar to open-ocean environments where there is no significant multipath). Fig. 4(a) depicts the output of Eq. 3 as a location probability heatpmap over 2D space, where yellow denotes higher probability of node location and navy blue represents lower probability. The red and pink stars represent the actual and estimated location and the error in localization is shown in the top right corner. We observe that the method works extremely well in the absence of multipath giving us a localization accuracy of 0.01m.

D. Backscatter Localization in Multipath Rich Environments

So far we have explored the application of underwater backscatter for localizing a node in deep water with minimal multipath interference, let us now examine its feasibility in shallow underwater environments. Fig. 4(b) shows a real scenario where the backscatter node was placed in a swimming pool. Unfortunately, the method outlined in §III-C proved ineffective in this scenario, resulting in a localization error of 2.68m. This error is predominantly due to multipath effects.

Multipath makes underwater localization challenging because the backscatter reflections are corrupted from the echoes coming from the air-water and water-sediment interfaces in such environments. Specifically, in shallow water environments (e.g., depth $\leq$ 4m), both the direct and reflected paths tend to have similar lengths, thereby resulting in comparable amplitudes. This similarity leads to interference between subsequent symbols (i.e., between different backscatter states). Failure to address this makes it hard to estimate the wireless channel (H_k) accurately and results in high localization error.

To mitigate this challenge, we leverage the *frequency-agnostic* characteristic of underwater backscatter by employing multiple frequencies instead of a single one. Specifically, when a backscatter node toggles its internal state between "reflective" and "non-reflective," it modulates all transmitted frequencies accordingly. 3D-BLUE uses this property by employing frequency hopping and estimates the channel $H_{i,k}$ for the k^{th} frequency and the i^{th} hydrophone receiver.

By exploiting the frequency-agnostic characteristic of underwater backscatter, 3D-BLUE can utilize not only spatial features but also spectral features for localization. Specifically, it can combine these features to achieve better localization accuracy in the presence of multipath, which is formulated as:

$$P(x,y,z) = \left|\left| \frac{1}{M}\frac{1}{N} \sum_{k=1}^{M}\sum_{i=1}^{N} H_{i,k} e^{\frac{-j2\pi d_i(x,y,z)}{\lambda_k}} \right|\right| \quad (4)$$

$$p_{node}(\hat{x},\hat{y},\hat{z}) = \arg\max_{(x,y,x)} P(x,y,z) \quad (5)$$

where M represents the number of transmitted frequencies. Fig. 4(c) and (d) depict scenarios where the number of frequencies was increased to 3 and 6 respectively. These heatmaps illustrate that increasing the frequencies substantially diminishes the error, enabling 3D-BLUE to accurately localize the backscatter node even in multipath-dense environments.

E. Underwater Localization under Mobility

In the previous section, we delved into how 3D-BLUE leverages spatial and spectral features to estimate the node's location in shallow water environments. While this algorithm demonstrates resilience to multipath in scenarios where the node remains stationary, it faces challenges when localizing a moving node. This difficulty stems from the dynamic nature of multipath reflections, which change over time as the node moves. Consequently, despite the incorporation of spatial and spectral features, the accuracy of the location estimate may

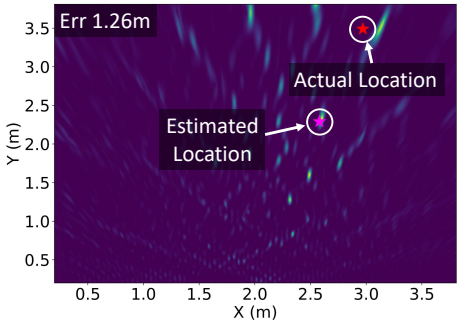

Fig. 5: **Localization under mobility.** The figure shows the sample heat map for a moving node in a shallow environment (without particle filter).

fluctuate. Fig. 5 shows a heatmap for the scenario where a node is moving in shallow water. We can observe that despite using multiple frequencies and hydrophones, the localization error increased from 5 cm (in the previous example) to 1.26 m.

To tackle this issue, one could theoretically add more frequencies and hydrophones. However, both options present drawbacks. The number of frequencies is constrained by the bandwidth of the underwater channel and the node itself, while increasing the number of hydrophones would increase the overall cost and size.

To address these challenges, 3D-BLUE incorporates temporal features by employing a particle filter-based algorithm. Fig. 6 illustrates our algorithm for robust location estimation. As described in Section §III-D, 3D-BLUE uses the probability heatmap P to find the location of the node from the peak. However, this is not the optimal strategy in the presence of changing multipath (i.e. mobility), which may lead to fictitious peaks around the true peak location, increasing the probabiltiy of location error. To solve this, 3D-BLUE refines the observation model and creates a new probability distribution P_n by constructing a mixture Gaussian using N Gaussians, where each Gaussian is centered at one of the peak locations $peak_i$ [1] in P and has a fixed variance of σ_p.[2] This can be expressed mathematically as:

$$P_n(r) = \sum_{i=1}^{N} \frac{1}{\sigma_p\sqrt{2\pi}} e^{-\frac{1}{2}\left(\frac{r-peak_i}{\sigma_p}\right)^2} \tag{6}$$

Since P_n combines different maxima from P, it contains the contribution from both the true location peak and erroneous peaks. 3D-BLUE uses P_n to iteratively narrow in on the true location and ignore the other erroneous peaks. It achieves this in three steps: in the first step, it creates another filter map P_f (initialized as all 1's) and projects it onto the mixture gaussian P_n to generate the location probability map P_l. The second step is the estimation step where 3D-BLUE obtains the location estimate by finding the coordinate (x^*, y^*, z^*) that maximizes P_l. Finally, in the update step 3D-BLUE moves the entire location map P_l in the same direction as the robot, using the velocity $v(x, y, x)$

[1]We selected $N = 60$ peaks that were separated by at least 4 cm. The number of peaks and minimum separation are hyperparameters.

[2]This is a hyperparameter that can be tuned, we experimented with different values and realized that a value of 50cm for σ_p gives the best performance

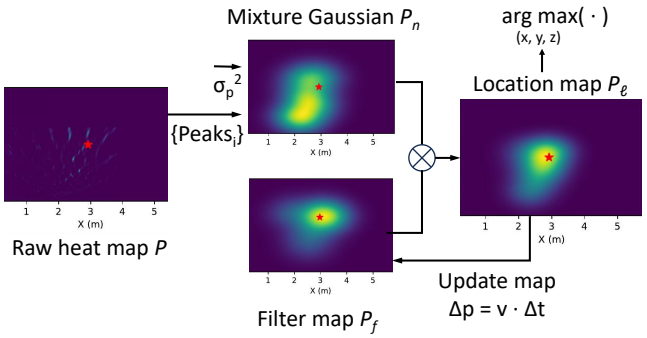

Fig. 6: **Robust Location Estimation using 3D-BLUE's Particle Filter.** Using the raw heat map P, 3D-BLUE generates a Gaussian mixture distribution P_n. It projects this distribution onto a filter map P_f and uses the output to obtain the location map P_l which it uses for location estimation. The location is updated with a motion model.

of the robot and the time interval Δt between samples [3]. 3D-BLUE then replaces the filter map P_f with the updated location map P_l^+ and repeats the process. Mathematically this can be expressed as:

1.) Projection Step: $P_l = P_n \cdot P_f$

2.) Estimation Step: $(x^*, y^*, z^*) = \arg\max_{(x,y,z)} P_l$

3.) Update Step: $P_l^+ = P_l + v(x, y, x)\Delta t$

$P_f \leftarrow P_l^+$

By incorporating temporal features from the motion model of the robot into the location estimation process, 3D-BLUE can iteratively narrow down on the true location peak and then consistently track the location of the robot with low error. Figure 7 illustrates how 3D-BLUE employs the particle filter to refine the location probability to a smaller area. The first row presents the raw heatmap P, while the second row depicts the corresponding mixture Gaussian heatmap P_n generated from P. The third row shows the evolution of the location map P_l. We make the following observations:

- The size of the yellow region in P_l (third row) decreases over time, indicating a reduction in 3D-BLUE's uncertainty regarding the location estimate.
- After applying the particle filter (third row of Figure 7), the error is significantly reduced compared to the other two rows, demonstrating the benefit of the particle filters.
- Interestingly, in some cases (e.g., column 1, row 2), simply applying the mixture of Gaussians from the projection step in the particle filter results in a significant reduction in error. This is because the Gaussians average out nearby estimates, increasing confidence in the mean of their corresponding locations which may be close to the true location.

F. From 2D to 3D

So far we discussed how 3D-BLUE can perform 2D localization in multipath rich underwater environments and under mobility. To extend this to 3D localization, one option is to create a 2D hydrophone array. However, such an approach would add cost and complexity to the system.

[3]This velocity can be obtained using an IMU sensor on the robot

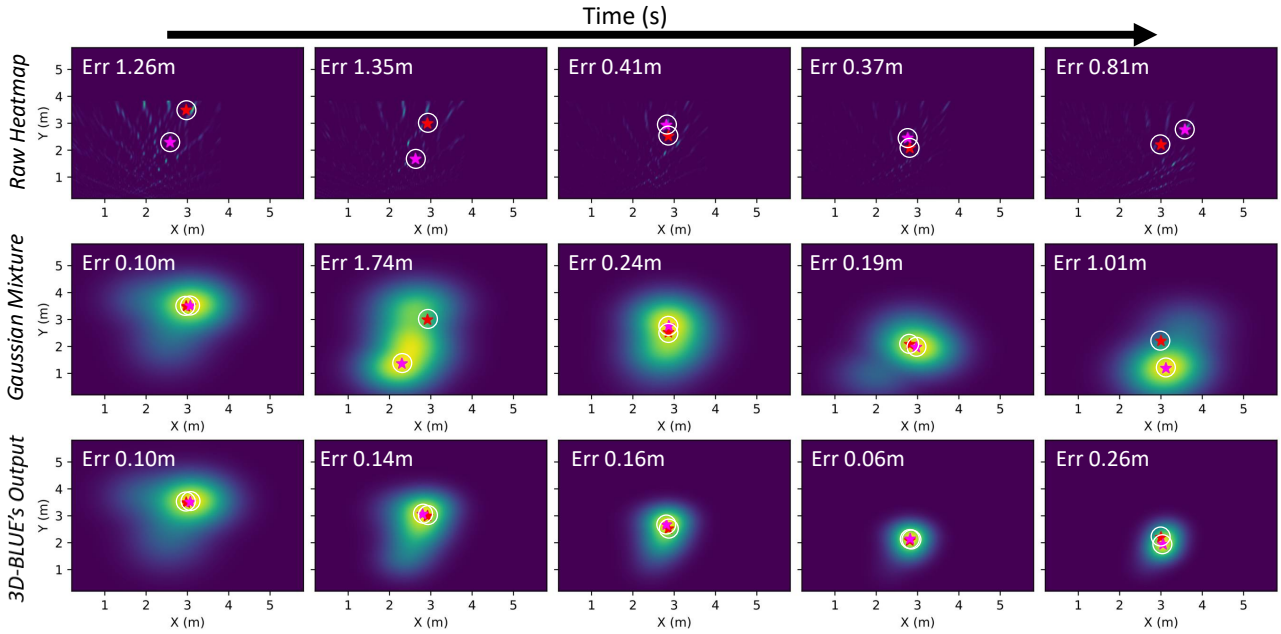

Fig. 7: **3D-BLUE's Particle Filter.** The figure plots the probability distribution of the robot's location as a heatmap over 2D space, where yellow and navy blue indicate highest and lowest probabilities respectively. Rows 1, 2 and 3 show the heatmaps of P, P_n, and P_l respectively vs time.

Instead, 3D-BLUE employs a pressure sensor to estimate the depth of the robot (corresponding to the z-axis location). Specifically, the estimated pressure can be converted to depth by accounting for water density. The obtained depth data is then transmitted to the base station, which incorporates it into the optimization framework (as outlined in equation 4) to search for the optimal (x,y) coordinates maximizing the received power P. This completes the loop for end-to-end 3D localization for 3D-BLUE.

IV. IMPLEMENTATION

Backscatter Node: The core of the backscatter node transducer is the SMC5447T40111 piezoceramic cylinder from Steminc, with a nominal resonance frequency of 17 kHz in radial mode. To fabricate the transducer, we followed a similar process to past work [14].

Transceiver: We use a similar transducer (as the backscatter node) as our transmitter. The transmitter node is connected to a class-D power amplifier TI TPA3245 through a high-power transformer matching network. The backscattered signal is received by a 8-element receiver hydrophone array which consists of 8 low-cost Aquarian Audio A5 hydrophones [33]. The received signal at each hydrophone is sampled by a 24-bit ADC Cirrus Logic CS5381.

UUV Platform: Our experiments were conducted using a BlueROV2 robot. It was controlled through a Mac Mini 2018 with 6-core Intel Core i5 processor, running Ubuntu 20.04 and ROS Noetic. We utilized the mavros library to send control commands to the BlueROV2 and interface with its onboard sensors. Additionally, we implemented a PID controller to enable the robot to either maintain a stationary position or follow a specified trajectory at a designated speed.

Ground Truth System: We developed our ground truth system based on vision-based techniques. The system includes AprilTags and the onboard camera of the BlueROV2. The AprilTags were printed in two sizes, 0.166m and 0.558m, to accommodate different ranges. The onboard camera is a low-light HD camera with a resolution of 2 Megapixels at 1080p. We integrated the AprilTag ROS wrapper to determine the positions of the AprilTags relative to the camera and conducted matrix transformations to map the UUV's location to the global frame. The locations computed served as the ground truth for our experiments. Note that the ground truth uses vision, which works well in our testing environment but not in rivers or lakes due to turbidity (see II).

V. RESULTS

We collected data for more than 1900 locations. This data is split in 25 experiments with a UUV to evaluate the localization accuracy of 3D-BLUE, and understand the impact of mobility, trajectory, array size, number of frequencies, and particle filter.

A. Range vs Accuracy

First, we analyzed the localization accuracy of 3D-BLUE at different ranges in Figure 8a. We evaluated 3D-BLUE from a range of 1.6m to 11m, both with and without the particle filter technique defined in Section §III-E. The blue and pink line represents the median 3D localization error with and without the use of a particle filter respectively. The error bars represent the 25^{th} and 75^{th} percentile respectively. Based on the results, we make the following remarks:

- 3D-BLUE outperforms its partial implementation counterpart without the particle filter in median localization error. As the range increases, the particle filter helps to smooth out erroneous location estimates and strengthens the weights of the estimates at the correct location. At ranges greater than 5m, the median error is reduced by an average of 0.82m. This proves that our system can provide more robust location estimates with a particle filter.

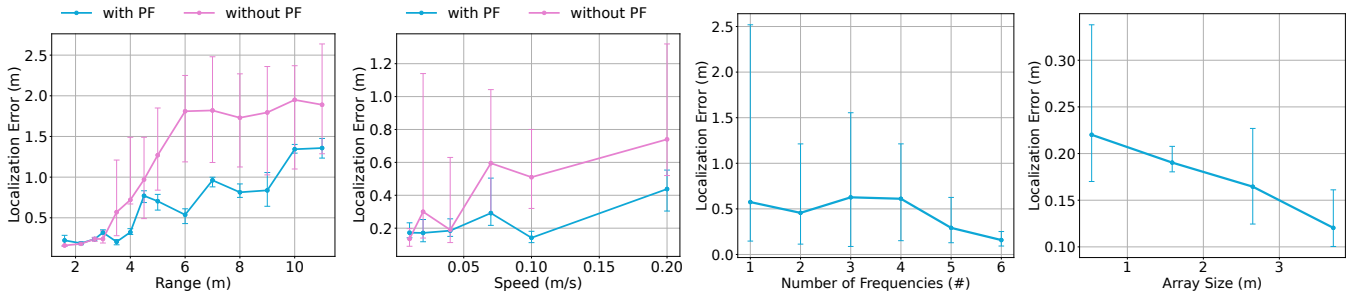

(a) Error vs Range (b) Error vs Robot Speed (c) Error vs Number of Freq (d) Error vs Array Size

Fig. 8: **3D-BLUE evaluation.** The figure shows the localization error of 3D-BLUE (in blue) vs (a) range, (b) speed, (c) number of frequencies, and (d) array size. The pink plots show the accuracy without the particle filter.

- 3D-BLUE is capable of achieving a localization error of less than 0.32m within a 4-meter range. Beyond this range, the median error continues to increase until it reaches 1.35m at a range of 11m.

- The limiting factor to the localization range of 3D-BLUE is the signal-to-noise ratio (SNR) of the backscattered signal received by the hydrophone array. The maximum range of a classical omnidirectional backscatter node (similar to that used by 3D-BLUE) is 11m. In the future, this range can be extended up to 150 m using more sophisticated retro-directive backscatter nodes [34] and applying the same algorithms developed in 3D-BLUE.

B. Accuracy under Mobility

We evaluated the localization accuracy of 3D-BLUE while the UUV was in motion. We predefined 8 trajectories with target speeds ranging from 0.01m/s to 0.2m/s. Figure 8b shows the localization error of 3D-BLUE at different robot movement speeds. Figure 9 shows three sample 3D trajectories of the UUV (both ground truth and estimated locations). We note the following:

- 3D-BLUE exhibits better median localization error compared to the implementation that does not use a particle filter. When the robot is moving at a target speed of 0.2m/s along the predefined trajectory, the median localization error is 0.43m. In contrast, the baseline without the particle filter presents a median localization error of 0.74m.

- 3D-BLUE is capable of achieving a low localization error when the UUV moves at a speed lower than 0.1m/s, with median errors all below 0.3m at speeds under 0.1m/s.

- Higher median localization errors are observed at higher speeds, e.g., 0.2m/s movement. This could be attributed to two factors: the displacement of the UUV's position at higher speeds, leading to larger errors within the 6-second location estimate period, and the non-negligible Doppler effect at higher speeds.

- 3D-BLUE's location estimates align with the ground truth, without accumulating errors like IMU, which means that loop trajectories can close without drift.

C. Number of Frequencies

We also evaluated 3D-BLUE with different number of frequencies. Figure 8c shows the mean localization error of 3D-BLUE with 10th and 95th percentile error bar as a function of different number of frequencies. The system's performance is assessed within a range of approximately 3m, both when the UUV is stationary and when it is in motion. All of the trials applied the particle filter.

Our results show that 3D-BLUE can obtain more robust and accurate location estimates with more frequencies. If 3D-BLUE only uses a single frequency, the 95th percentile localization error is 2.52m, and the mean error is 0.57m. However, as we start incorporating more frequencies, the 95th percentile localization error decreases. When 3D-BLUE uses 6 frequencies, the 95th percentile localization error is 0.25m, and the mean error is 0.15m. This indicates that 3D-BLUE can achieve more accurate location estimates with more frequencies.

D. Hydrophone Array Size

We explored the impact of array size on the localization error of 3D-BLUE. Figure 8d displays the median localization error with error bars for the 25th and 75th percentiles across different array sizes. The system's performance is assessed within a range of around 3m, both when the UUV is stationary and when it is in motion. The particle filter was applied in all trials.

Our results show that larger array size results in a lower localization error. Longer hydrophone arrays can provide greater spatial diversity for the measurements, which reduces both the error and the variance in location estimates. At an array size of 3.71m, the median error is 0.12m, with the 25th and 75th percentiles at 0.1m and 0.16m.

VI. DISCUSSION & CONCLUSION

3D-BLUE is an ultra-low-power underwater 3D localization system designed for compact robots in shallow underwater environments. Unlike previous localization systems which were tailored primarily for larger/more-powerful marine robots in low-multipath environments, 3D-BLUE introduces multiple innovations to enable ultra-low-power accurate localization of compact robotics in shallow-water environments. By integrating temporal, spatial, and spectral features of acoustic backscatter, 3D-BLUE achieves high localization accuracy even in environments with rich multipath. As the research evolves, it would be interesting to extend it to longer ranges using more sophisticated backscatter designs [34]; explore sensor fusion (acoustic-visual) methods that combine acoustic backscatter with VIO for localization;

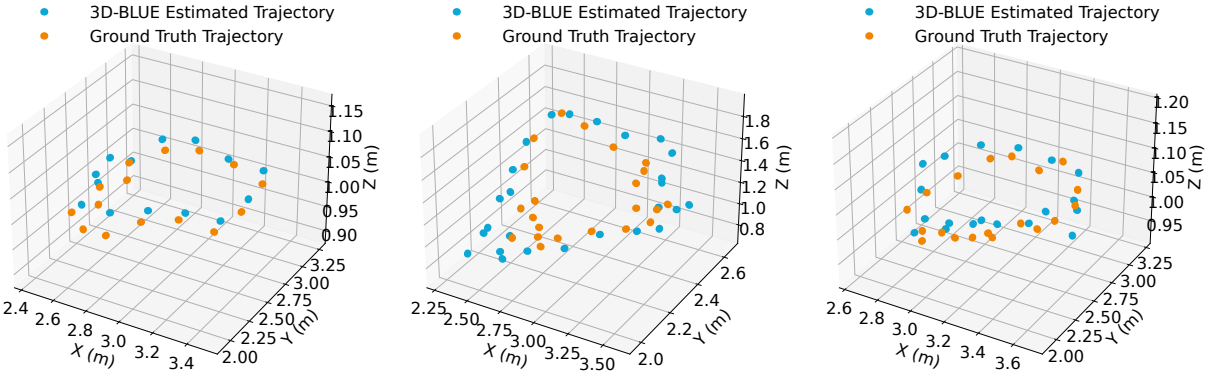

(a) Trajectory 1 (b) Trajectory 2 (c) Trajectory 3

Fig. 9: **Robot Trajectory.** The figure plots the robot trajectory while it moves in 3D space (a) and (c) plot the scenario when the robot moves in X-Y plane, however (b) plots the case when the robot moves in the X-Z plane. Blue and orange dots represent the estimated and ground truth locations.

develop advanced signal processing techniques to deal with Doppler at higher speeds; and integrate this method on swarms of micro-robots where its ultra-low-power would be even more instrumental. More generally, it would be valuable to apply this technology for various commercial, naval, and environmental UUV-based monitoring applications.

REFERENCES

[1] "Underwater drone market 2023 to 2030." https://www.linkedin.com/pulse/underwater-drone-market-2023-2030-size-share-xewlf/.

[2] S. Halder and K. Afsari, "Robots in inspection and monitoring of buildings and infrastructure: A systematic review," *Applied Sciences*, vol. 13, no. 4, p. 2304, 2023.

[3] J. Luo, Z. Qian, L. Gui, M. Zhang, and X. Geng, "Design and implementation of pollution monitoring system in waterway area based on bionic robotic fish," in *ISCCN 2022*, vol. 12332, pp. 90–94, SPIE, 2022.

[4] D. S. Terracciano, L. Bazzarello, A. Caiti, R. Costanzi, and V. Manzari, "Marine robots for underwater surveillance," *Current Robotics Reports*, vol. 1, pp. 159–167, 2020.

[5] S. B. Williams, O. R. Pizarro, M. V. Jakuba, C. R. Johnson, N. S. Barrett, R. C. Babcock, G. A. Kendrick, P. D. Steinberg, A. J. Heyward, P. J. Doherty, *et al.*, "Monitoring of benthic reference sites: using an autonomous underwater vehicle," *IEEE Robotics & Automation Magazine*, vol. 19, no. 1, pp. 73–84, 2012.

[6] Y. Han, C. Zheng, and D. Sun, "Accurate underwater localization using lbl positioning system," in *OCEANS 2015-MTS/IEEE Washington*, pp. 1–4, IEEE, 2015.

[7] G. Cario, A. Casavola, G. Gagliardi, M. Lupia, and U. Severino, "Accurate localization in acoustic underwater localization systems," *Sensors*, vol. 21, no. 3, p. 762, 2021.

[8] F. Mandić, I. Rendulić, N. Mišković, . Na, *et al.*, "Underwater object tracking using sonar and usbl measurements," *Journal of Sensors*, vol. 2016, 2016.

[9] L. Whitcomb, D. R. Yoerger, H. Singh, and J. Howland, "Advances in underwater robot vehicles for deep ocean exploration: Navigation, control, and survey operations," in *Robotics Research: The Ninth International Symposium*, pp. 439–448, Springer, 2000.

[10] D. R. Yoerger, A. M. Bradley, B. Walden, M. Cormier, and W. Ryan, "High resolution mapping of a fast spreading mid ocean ridge with the autonomous benthic explorer," in *International Symposium on Unmanned Untethered Submersible Technology*, pp. 21–31, UNIVERSITY OF NEW HAMPSHIRE-MARINE SYSTEMS, 1999.

[11] H.-P. Tan, R. Diamant, W. K. Seah, and M. Waldmeyer, "A survey of techniques and challenges in underwater localization," *Ocean Engineering*, vol. 38, no. 14-15, pp. 1663–1676, 2011.

[12] "UrbanDrones.com - USBL for Chasing M2 Pro Underwater Drone."

[13] "Blueskiesdroneshop.com - Chasing Gladius Mini S ROV (200m)."

[14] J. Jang and F. Adib, "Underwater backscatter networking," in *Proceedings of the ACM Special Interest Group on Data Communication*, pp. 187–199, 2019.

[15] W. Wang, J. Liu, G. Xie, L. Wen, and J. Zhang, "A bio-inspired electrocommunication system for small underwater robots," *Bioinspiration & biomimetics*, vol. 12, no. 3, p. 036002, 2017.

[16] H. Huang and Y. R. Zheng, "Node localization with aoa assistance in multi-hop underwater sensor networks," *Ad hoc networks*, vol. 78, pp. 32–41, 2018.

[17] Y. Sun, Y. Yuan, Q. Xu, C. Hua, and X. Guan, "A mobile anchor node assisted rssi localization scheme in underwater wireless sensor networks," *Sensors*, vol. 19, no. 20, p. 4369, 2019.

[18] "iXblue - RAMSES Underwater Acoustic System."

[19] "Water Linked - Underwater GPS G2."

[20] "Advanced Navigation - Subsonus USBL System."

[21] X. Tan and J. Li, "Cooperative positioning in underwater sensor networks," *IEEE Transactions on Signal Processing*, vol. 58, no. 11, pp. 5860–5871, 2010.

[22] E. Dubrovinskaya, R. Diamant, and P. Casari, "Anchorless underwater acoustic localization," in *2017 WPNC*, pp. 1–6, 2017.

[23] K.-C. Lee, J.-S. Ou, M.-C. Huang, and M.-C. Fang, "A novel location estimation based on pattern matching algorithm in underwater environments," *Applied Acoustics*, vol. 70, no. 3, pp. 479–483, 2009.

[24] C. O. Tiemann, M. B. Porter, and L. N. Frazer, "Localization of marine mammals near hawaii using an acoustic propagation model," *The Journal of the Acoustical society of America*, vol. 115, no. 6, pp. 2834–2843, 2004.

[25] R. Ghaffarivardavagh, S. S. Afzal, O. Rodriguez, and F. Adib, "Underwater backscatter localization: Toward a battery-free underwater gps," in *Proceedings of the 19th ACM Workshop on Hot Topics in Networks*, HotNets '20, (New York, NY, USA), p. 125–131, Association for Computing Machinery, 2020.

[26] S. S. da Costa Botelho, P. Drews, G. L. Oliveira, and M. da Silva Figueiredo, "Visual odometry and mapping for underwater autonomous vehicles," in *2009 6th Latin American Robotics Symposium (LARS 2009)*, pp. 1–6, IEEE, 2009.

[27] S. Hu, J. Tang, Z. Ren, C. Chen, C. Zhou, X. Xiao, and T. Zhao, "Multiple underwater objects localization with magnetic gradiometry," *IEEE Geoscience and Remote Sensing Letters*, vol. 16, no. 2, pp. 296–300, 2018.

[28] D. Kim, D. Lee, H. Myung, and H.-T. Choi, "Artificial landmark-based underwater localization for auvs using weighted template matching," *Intelligent Service Robotics*, vol. 7, pp. 175–184, 2014.

[29] T. Zhao, J. Tang, S. Hu, G. Lu, X. Zhou, and Y. Zhong, "State-transition-algorithm-based underwater multiple objects localization with gravitational field and its gradient tensor," *IEEE Geoscience and Remote Sensing Letters*, vol. 17, no. 2, pp. 192–196, 2019.

[30] P. Corke, C. Detweiler, M. Dunbabin, M. Hamilton, D. Rus, and I. Vasilescu, "Experiments with underwater robot localization and tracking," in *ICRA 2007*, pp. 4556–4561, IEEE, 2007.

[31] Y. Ma, N. Selby, and F. Adib, "Minding the billions: Ultrawideband localization for deployed rfid tags," *ACM MobiCom*, 2017.

[32] F. Adib, C.-Y. Hsu, H. Mao, D. Katabi, and F. Durand, "Capturing the human figure through a wall," *ACM TOG*, 2015.

[33] "H1C Hydrophone." https://www.aquarianaudio.com.

[34] A. Eid, J. Rademacher, W. Akbar, P. Wang, A. Allam, and F. Adib, "Enabling long-range underwater backscatter via van atta acoustic networks," in *ACM SIGCOMM 2023*, pp. 1–19, 2023.